


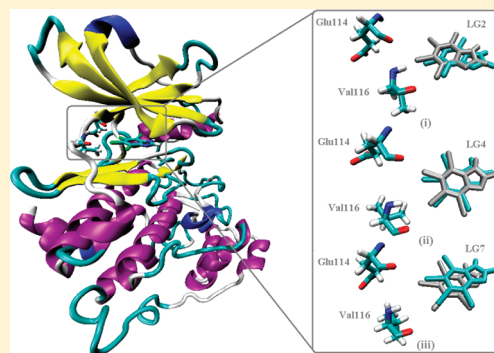
Performance Assessment of Semiempirical Molecular Orbital Methods in Describing Halogen Bonding: Quantum Mechanical and Quantum Mechanical/Molecular Mechanical-Molecular Dynamics Study

Mahmoud A. A. Ibrahim*

School of Chemistry, University of Manchester, Oxford Road, Manchester M139PL, United Kingdom
Chemistry Department, Faculty of Science, Minia University, Minia 61519, Egypt

 Supporting Information

ABSTRACT: The performance of semiempirical molecular-orbital methods—MNDO, MNDO-*d*, AM1, RM1, PM3 and PM6—in describing halogen bonding was evaluated, and the results were compared with molecular mechanical (MM) and quantum mechanical (QM) data. Three types of performance were assessed: (1) geometrical optimizations and binding energy calculations for 27 halogen-containing molecules complexed with various Lewis bases (Two of the tested methods, AM1 and RM1, gave results that agree with the QM data.); (2) charge distribution calculations for halobenzene molecules, determined by calculating the solvation free energies of the molecules relative to benzene in explicit and implicit generalized Born (GB) solvents (None of the methods gave results that agree with the experimental data.); and (3) appropriateness of the semiempirical methods in the hybrid quantum-mechanical/molecular-mechanical (QM/MM) scheme, investigated by studying the molecular inhibition of CK2 protein by eight halobenzimidazole and -benzotriazole derivatives using hybrid QM/MM molecular-dynamics (MD) simulations with the inhibitor described at the QM level by the AM1 method and the rest of the system described at the MM level. The pure MM approach with inclusion of an extra point of positive charge on the halogen atom approach gave better results than the hybrid QM/MM approach involving the AM1 method. Also, in comparison with the pure MM-GBSA (generalized Born surface area) binding energies and experimental data, the calculated QM/MM-GBSA binding energies of the inhibitors were improved by replacing the $G_{\text{GB,QM/MM}}$ solvation term with the corresponding $G_{\text{GB,MM}}$ term.



INTRODUCTION

Noncovalent interactions are of great importance in studies on crystal design and drug discovery.^{1–6} One such noncovalent interaction, halogen bonding, is present between a covalently bound halogen atom and a Lewis base.^{7–9} A halogen bond is a directional interaction caused by the anisotropic distribution of charge on a halogen atom *X*, which in turn forms a positive region called a σ -hole on the A–*X* axis.^{7–9} Numerous theoretical and experimental studies have been carried out to better understand the properties of halogen bonding in crystal structures and biological systems.^{2,3,7,8,10–17}

The lack of a molecular-mechanical (MM) force field with respect to the anisotropic charge distribution on the halogen atom is an obstacle in molecular-dynamics (MD) studies of halogen bonding in biological systems.^{3,18} One approach that has been proposed to address this problem is to represent the positive cap on a halogen atom with an extra-point of positive charge in MM potentials.¹⁸ The hybrid quantum-mechanical/molecular-mechanical (QM/MM) technique is another useful approach to describe ligand–charge polarization.^{19,20} In QM/MM-MD, the inhibitor is described at the QM level, often by a semiempirical method, resulting in a better charge description.

The protein, including solvent molecules, is described using a MM force field.

Semiempirical methods have been used widely over the last decades in studies ranging from geometry optimizations and molecular modeling to reproduction of physical data such as heat of formation, proton affinity, spectroscopic parameters, and reaction energies.^{21–28} Semiempirical methods are popular because of their relatively modest time and computational costs compared with QM methods and their relative ease of applicability for study of reactive processes at active sites compared with MM force field methods.^{29–32} Semiempirical methods have also been studied in detail; for example, the accuracies of semiempirical electrostatic potentials and potential-derived charges^{33–42} and the appropriateness of these methods in treating QM/MM interactions^{19,43} have been evaluated. However, to our knowledge, no studies have yet been reported that assess the performance of semiempirical methods in describing noncovalent halogen bonding.

Received: June 10, 2011

Published: September 26, 2011

Table 1. Parameters Used for the Extra Point of Positive Charge

parameter	value
mass (EP)	0.00 amu
r^* (EP)	1.00 Å
ε (EP)	0.00 Å
r_{eq} (Cl-EP)	1.95 Å
r_{eq} (Br-EP)	2.22 Å
r_{eq} (I-EP)	2.35 Å
K_r (X-EP) ^a	600.0
Θ_{eq} (A-X-EP) ^a	180.0°
K_θ (A-X-EP) ^a	150.0
γ (A-A-X-EP) ^a	0.00°
V_n (A-A-X-EP) ^a	0.00

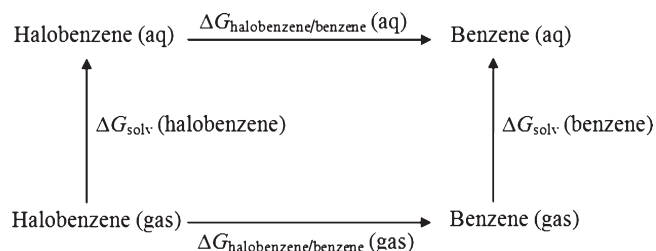
^aX = Cl, Br, or I.

In the current study, the accuracy of semiempirical methods in describing halogen bonding was assessed by examining the three types of performance. First, geometrical optimizations and binding energy calculations for 27 halogen-containing complexes were performed using six semiempirical methods and the results were compared with MM and QM data. Second, the solvation free energies of halobenzene molecules relative to benzene were calculated in explicit and implicit solvents, to examine the accuracy of the semiempirical charge distributions. Finally, the most promising of the tested methods, AM1, was used to perform MD simulations of the molecular inhibition of protein kinase CK2, to evaluate the reliability of semiempirical method in describing the halogen bonding in the hybrid QM/MM scheme. CK2 is a multifunctional Ser/Thr protein that is involved in several physiological and pathological processes.⁴⁴ Polyhalogenobenzimidazole and -benzotriazole compounds are reportedly potent inhibitors of CK2^{45–51} and act by forming halogen bonds with the hinge region of CK2.^{46–48,52} The binding energies of eight halobenzimidazole and -benzotriazole inhibitors with CK2 were calculated using hybrid QM/MM-MD simulations combined with generalized Born surface area (GBSA) calculations; the inhibitor was described at the QM level using AM1 method and the rest of the system was described at the MM level. The results were then compared with those obtained by pure MM-MD simulations and with experimental data.

METHODS

Molecular Optimization. The test set for this study was the same as that for our previous MM study on halogen bonding.¹⁸ The test set contained 27 halogen-containing molecules complexed with various Lewis bases. The complexes were optimized by the following six semiempirical molecular-orbital (MO) methods: MNDO,^{53,54} MNDO-*d*,^{55,56} AM1,^{57,58} RM1,⁵⁹ PM3,⁶⁰ and PM6.⁶¹ All semiempirical calculations were performed using MOPAC2009 software.⁶²

The semiempirical results were compared with density functional theory (DFT) and MM data from our previous study.¹⁸ For the DFT calculations, the B3LYP functional^{63,64} was used for bromine- and iodine-containing complexes, and the MPWLYP functional^{64,65} was used for chlorine-containing complexes, where the B3LYP functional gives an extremely long Cl...Lewis base contact.⁶⁶ A mixed basis set scheme was used; the aug-cc-pVDZ-PP^{67,68} was used to describe bromine and iodine atoms, and the 6-311+G**⁶⁹ basis

**Figure 1.** Thermodynamic cycle used to calculate the solvation free energy $\Delta\Delta G_{\text{solv}}$ of halobenzene molecule relative to benzene.

set was used to describe all other atoms, including chlorine atom. For the MM calculations, an extra point of positive charge was placed on the halogen atom at the atomic radius r^* ,¹⁸ and the partial charges were assigned using the restrained electrostatic-potential (RESP) approach.⁷⁰ The extra-point parameters, listed in Table 1, were taken from our previous study.¹⁸ Single-point energies were calculated at the semiempirical//semiempirical, MM//MM, DFT/6-311+G**//DFT/6-311+G**, and MP2/6-311+G**//DFT/6-311+G** levels of theory using the aug-cc-pVDZ-PP basis set for bromine and iodine atoms. All MM and DFT calculations were performed using the Gaussian 03 package.⁷¹

Relative Solvation Free Energy. The solvation free energy of the halobenzene molecules relative to benzene was calculated by the thermodynamic integration (TI) method^{72,73} implemented in AMBER software.⁷⁴ In the TI calculations, mutation of a halogen atom of the halobenzene molecule to a charged hydrogen atom was performed via the coupling parameter λ . TI simulations were performed for 500 ps in the gas phase with explicit and implicit generalized Born (GB) water solvents at $\lambda = 0.1127, 0.50$, and 0.88729 . The simulations were repeated at different levels to characterize the halobenzene and benzene molecules: MM, MNDO, AM1, RM1, and PM3 levels. For the MM calculations, the developed approach of including an extra point of positive charge on the halogen atom was applied.¹⁸

Before data collection, the molecular systems were energy-minimized, heated, and equilibrated over 150 ps. The time step was 1 fs and the SHAKE option was applied to constrain all water-hydrogen bonds. Free energy change ΔG was calculated by Gaussian-quadrature integration of the formula:

$$\Delta G = \int_0^1 \left\langle \frac{\partial V}{\partial \lambda} \right\rangle_\lambda d\lambda \approx \sum_i^n w_i \left\langle \frac{\partial V}{\partial \lambda} \right\rangle_{\lambda_i}$$

where the brackets denote the ensemble average, w_i is the weight coefficient for the i th-quadrature root point and $\partial V/\partial \lambda$ is the mixed potential function at the value of λ . Gaussian-quadrature points and weights were taken from the AMBER manual.⁷⁴ The relative solvation free energy $\Delta\Delta G_{\text{solv}}$ was calculated using the thermodynamic cycle shown in Figure 1 and given by

$$\begin{aligned} \Delta\Delta G_{\text{solv}} &= \Delta G_{\text{solv}}(\text{benzene}) - \Delta G_{\text{solv}}(\text{halobenzene}) \\ &= \Delta G_{\text{halobenzene/benzene}}(\text{aq}) - \Delta G_{\text{halobenzene/benzene}}(\text{gas}) \end{aligned}$$

MD Simulations. The performance of the most promising of the studied semiempirical methods, AM1, in describing halogen bonding in hybrid QM/MM scheme was further assessed by performing MD simulations of the molecular inhibition of CK2 protein with halobenzimidazole and -benzotriazole inhibitors.

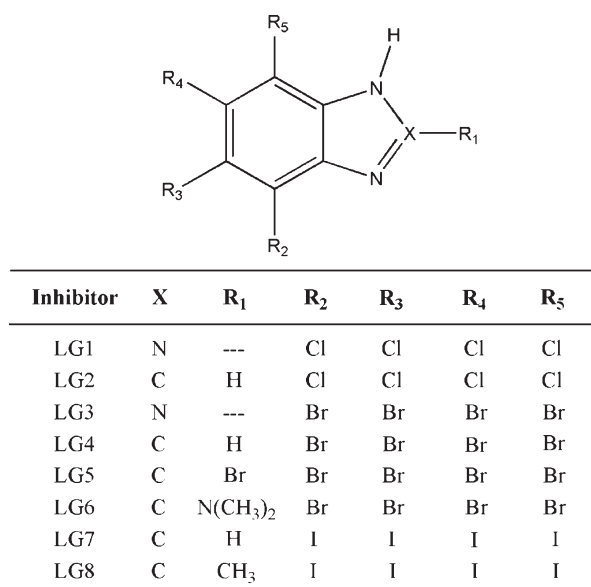


Figure 2. Chemical structure of the studied inhibitors against CK2 protein.

The results were then compared with those obtained by pure MM-MD simulations and with experimental data.

Figure 2 shows the chemical structures of the studied halogenated inhibitors. The crystal structure of CK2 complexed with 4,5,6,7-tetrabromo-*N,N*-dimethyl-1*H*-benzeneimidazol-2-amine (LG6) (PDB ID: 1ZOE)⁴⁶ was taken as the template for constructing the other molecular systems. The molecular systems were solvated with TIP3P water molecules.⁷⁵

Pure MM-MD and hybrid QM/MM-MD simulations were performed using the AMBER software.⁷⁴ For the MM-MD simulations, the general AMBER force field (GAFF)⁷⁶ was used to describe all the studied inhibitors, and AMBER force field 99SB⁷⁷ was used to describe the protein and solvent molecules. An extra point of positive charge was placed on each halogen atom of the inhibitors according to the parameters given in Table 1, and the partial charges of the inhibitors were estimated using the RESP approach.⁷⁰ For the QM/MM-MD simulations, the semiempirical AM1 method was used to describe the inhibitors, and AMBER force field 99SB was used to describe the rest of the system, including solvent molecules.

During the simulations, all molecular systems were energy-minimized, heated gradually over a period of 50 ps to 300 K, and equilibrated for 500 ps. For the MD simulations, a time step of 2 fs and the SHAKE option to constrain all bonds involving hydrogen atoms were used.

GBSA Binding Energy Calculations. The binding energies of the studied inhibitors with CK2 protein were calculated using MM-GBSA and QM/MM-GBSA approaches based on uncorrelated snapshots collected every 10 ps over the 2 ns production run from MM-MD and QM/MM-MD simulations, respectively.

For the MM-GBSA calculations, binding energy ΔG was calculated and average free energy \bar{G} was estimated by the following relationships:

$$\Delta G = \bar{G}_{\text{complex}} - (\bar{G}_{\text{receptor}} + \bar{G}_{\text{inhibitor}})$$

$$\bar{G} = \bar{E}_{\text{int}} + \bar{E}_{\text{vdw}} + \bar{E}_{\text{elec}} + \bar{G}_{\text{GB}} + \bar{G}_{\text{SA}} - TS$$

where \bar{G}_{GB} is the electrostatic solvation free energy calculated from

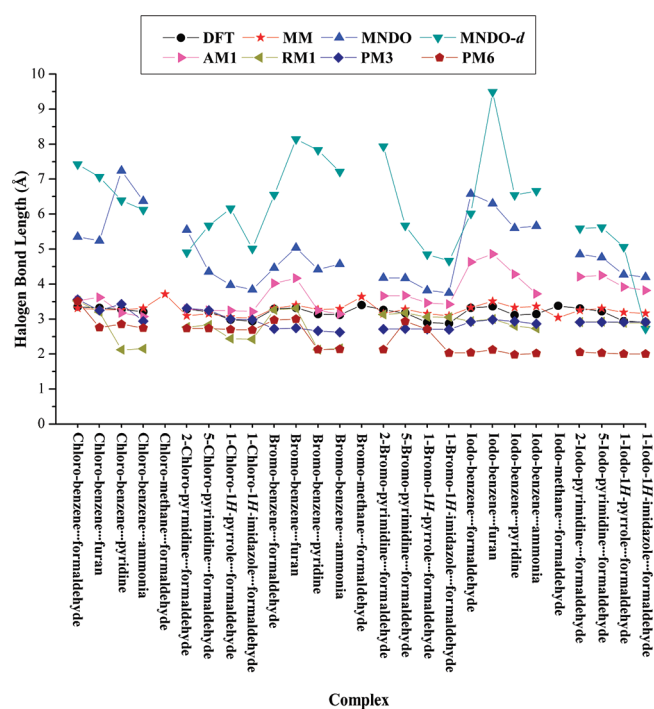


Figure 3. Calculated halogen bond lengths (Å) of the studied halogen-containing complexes.

the generalized Born equation $\bar{G}_{\text{GB}} = \bar{G}_{\varepsilon=78.3} - \bar{G}_{\varepsilon=1}$ and \bar{G}_{SA} is the nonpolar contribution to the solvation free energy from the solvent-accessible surface area (SASA). The latter is calculated from the relationship $\bar{G}_{\text{SA}} = \gamma \times \text{SASA} + \beta$, where γ and β are empirical constants set to 0.00542 and 0.92 kcal/mol, respectively.⁷⁸ In the current study, the inhibitor molecules were assumed to be rigid, and solute entropy was neglected.

For all of the GBSA calculations, a single-trajectory approach was used, in which the coordinates of each inhibitor, receptor, and complex were extracted from a single trajectory, causing the internal energy term to cancel out and binding energy ΔG to become

$$\Delta G = \Delta \bar{E}_{\text{vdw}} + \Delta \bar{E}_{\text{elec}} + \Delta \bar{G}_{\text{GB}} + \Delta \bar{G}_{\text{SA}}$$

For the QM/MM-GBSA calculations, the inhibitor was described at the QM level using the semiempirical AM1 method, and the rest of the system was described at the MM level. Binding energy ΔG was calculated by the following relationship

$$\Delta G = \Delta \bar{E}_{\text{vdw}} + \Delta \bar{E}_{\text{elec}} + \Delta \bar{E}_{\text{QM}} + \Delta \bar{G}_{\text{GB}} + \Delta \bar{G}_{\text{SA}}$$

where the \bar{E}_{QM} term in the implicit GB solvent calculation is technically the QM energy of the isolated QM region plus part of the solvation energy of the QM region. Therefore, the solvation energy contribution of QM energy can be split by modifying the \bar{G}_{GB} and \bar{E}_{QM} terms as follows:

$$\bar{G}_{\text{GB}} = \bar{G}_{\text{GB}} + \bar{E}_{\text{QM, solv}} + \bar{E}_{\text{QM, gas}}$$

$$\bar{E}_{\text{QM}} = \bar{E}_{\text{QM, gas}}$$

RESULTS AND DISCUSSION

Geometrical Optimizations and Binding Energy Calculations. Semiempirical level studies of halogen-bond-forming

Table 2. Calculated Halogen Bond Lengths of the 27 Studied Halogenated Complexes

complex	halogen bond length (Å)							
	DFT ^{a,b}	MM ^b	MNDO	MNDO- <i>d</i>	AM1	RM1	PM3	PM6
chlorobenzene...formaldehyde	3.35	3.31	5.35	7.42	3.53	3.52	3.56	3.51
chlorobenzene...furan	3.32	3.27	5.24	7.06	3.62	3.20	3.25	2.76
chlorobenzene...pyridine	3.27	3.26	7.24	6.39	3.17	2.12	3.43	2.85
chlorobenzene...ammonia	3.21	3.31	6.37	6.12	3.07	2.15	2.94	2.74
chloromethane...formaldehyde ^c	—	3.71	—	—	—	—	—	—
2-chloropyrimidine...formaldehyde	3.28	3.09	5.55	4.90	3.28	2.77	3.31	2.73
5-chloropyrimidine...formaldehyde	3.21	3.15	4.35	5.67	3.25	2.83	3.25	2.73
1-chloro-1 <i>H</i> -pyrrole...formaldehyde	2.98	3.05	3.97	6.16	3.24	2.44	3.00	2.70
1-chloro-1 <i>H</i> -imidazole...formaldehyde	2.94	3.02	3.84	5.01	3.21	2.42	2.98	2.69
rms for chloro complexes ^d		0.26	6.46	8.47	0.54	1.86	0.39	1.19
bromobenzene...formaldehyde	3.29	3.3	4.46	6.55	4.02	3.26	2.72	2.97
bromobenzene...furan	3.32	3.4	5.04	8.14	4.17	3.30	2.74	3.00
bromobenzene...pyridine	3.14	3.27	4.42	7.83	3.25	2.12	2.66	2.13
bromobenzene...ammonia	3.12	3.29	4.57	7.21	3.14	2.16	2.62	2.14
bromomethane...formaldehyde	3.4	3.64	—	—	—	—	—	—
2-bromopyrimidine...formaldehyde	3.26	3.15	4.18	7.93	3.66	3.13	2.71	2.13
5-bromopyrimidine...formaldehyde	3.17	3.28	4.17	5.67	3.67	3.17	2.72	2.93
1-bromo-1 <i>H</i> -pyrrole...formaldehyde	2.9	3.15	3.82	4.85	3.46	3.06	2.71	2.71
1-bromo-1 <i>H</i> -imidazole...formaldehyde	2.87	3.09	3.75	4.66	3.42	3.05	2.70	2.03
rms for bromo complexes ^d		0.43	3.39	10.37	1.52	1.42	1.31	2.07
iodobenzene...formaldehyde	3.32	3.33	6.58	6.01	4.63	2.94	2.92	2.04
iodobenzene...furan	3.36	3.51	6.30	9.49	4.86	3.00	2.98	2.12
iodobenzene...pyridine	3.11	3.33	5.60	6.54	4.28	2.80	2.93	1.98
iodobenzene...ammonia	3.14	3.36	5.66	6.66	3.72	2.73	2.86	2.02
iodomethane...formaldehyde	3.38	3.04	—	—	—	—	—	—
2-iodopyrimidine...formaldehyde	3.3	3.25	4.85	5.59	4.21	2.91	2.91	2.05
5-iodopyrimidine...formaldehyde	3.22	3.3	4.76	5.62	4.25	2.92	2.91	2.03
1-iodo-1 <i>H</i> -pyrrole...formaldehyde	2.94	3.19	4.27	5.06	3.92	2.89	2.91	2.00
1-iodo-1 <i>H</i> -imidazole...formaldehyde	2.91	3.16	4.20	2.72	3.82	2.88	2.91	2.00
rms for iodo complexes ^d		0.50	6.33	9.20	3.05	1.42	0.81	3.23
total rms ^d		0.71	9.65	16.25	3.45	2.50	1.59	4.01

^a Different DFT functionals were used: B3LYP functional for bromo and iodo complexes, PMWLYP functional for chloro complexes, and mixed basis set scheme (aug-cc-pVDZ-PP basis set for the iodine and bromine atoms and 6-311+G** for all the other atoms). ^b Taken from our previous study.¹⁸ ^c No halogen bond formed.⁹ ^d Halomethane complex was not included in the rms estimation.

complexes have not heretofore been reported in the literature. In the current study, the molecular structures of halogenated molecules that form halogen bonds with various Lewis bases were optimized by MNDO, MNDO-*d*, AM1, RM1, PM3, and PM6 semiempirical methods.

Figure 3 shows plots of the calculated minimized halogen bond lengths of the complexes. For comparison, the corresponding calculated MM and DFT lengths are also included; the latter are taken from our previous study.¹⁸ The calculated halogen bond lengths and energies are presented in Tables 2 and 3.

Molecular optimizations of the studied complexes by the MNDO and MNDO-*d* methods give very long halogen...Lewis base contact distances and positive binding energies, suggesting that no halogen bond has formed between the halogen atom and Lewis base.

Molecular optimization of the studied complexes by the AM1 method gives the following halogen bond lengths and binding energies. AM1 bond lengths for the chloro and bromo complexes are consistent with the corresponding DFT data, with rms error

of 0.54 and 1.52 Å, respectively. AM1 bond lengths for the iodo complexes, however, are long relative to the corresponding DFT data, with rms error of 3.05 Å. AM1 binding energies for all the complexes are low relative to the corresponding DFT data. The AM1 iodo halogen bond energy is also low relative to the corresponding bromo halogen bond energy, presumably because of the longer length of the iodo halogen bond. The unsigned rms errors of the AM1 halogen bond energies relative to the corresponding DFT data are 1.78, 2.93, and 6.62 kcal/mol for the chloro, bromo, and iodo complexes, respectively.

The RM1 method is a reparameterization of the AM1 method based on geometry optimization, heat of formation, and binding energy calculations.⁵⁹ Thus, it would be expected to give better results than the AM1 method. Indeed, for chlorobenzene complexed with formaldehyde and furan, the RM1 halogen bond length obtained is slightly closer to the corresponding DFT data than the AM1 halogen bond length. However, for the other studied chloro complexes, the RM1 bond lengths are short relative to the corresponding DFT data, with rms error of 1.86 Å.

Table 3. Calculated Halogen Bond Energies of the 27 Studied Halogenated Complexes

complex	binding energy ^a (kcal/mol)								
	DFT ^{b,c}	MP2 ^{b,d}	MM ^b	MNDO	MNDO-d	AM1	RM1	PM3	PM6
chlorobenzene...formaldehyde	−0.30	−0.79	−0.30	0.23	0.13	0.07	0.17	0.22	0.21
chlorobenzene...furan	−0.73	−1.90	−0.75	0.10	0.05	0.01	−0.15	0.42	−1.19
chlorobenzene...pyridine	−0.86	−2.28	−0.95	0.13	0.18	−0.29	−4.63	0.22	−0.63
chlorobenzene...ammonia	−0.90	−1.30	−0.47	0.16	0.19	−0.43	−7.30	0.39	−1.09
chloromethane...formaldehyde ^e	—	—	0.50	—	—	—	—	—	—
2-chloropyrimidine...formaldehyde	−0.35	−0.82	−0.82	0.20	0.29	−0.13	−0.58	0.03	−1.75
5-chloropyrimidine...formaldehyde	−1.03	−1.63	−1.10	0.00	0.02	−0.45	−0.97	−0.31	−2.11
1-chloro-1H-pyrrole...formaldehyde	−1.90	−2.62	−2.09	−0.37	0.08	−1.01	−2.30	−0.56	−2.92
1-chloro-1H-imidazole...formaldehyde	−2.19	−3.02	−2.74	−0.60	−0.17	−1.30	−2.80	−0.94	−3.44
rms for chloro complexes relative to DFT ^f			0.87	3.06	3.54	1.78	7.50	2.91	2.51
rms for chloro complexes relative to MP2 ^f			2.16	5.26	5.68	4.06	6.79	5.16	2.38
bromobenzene...formaldehyde	−0.37	−1.68	−1.35	0.09	0.15	0.00	−0.32	−1.62	−1.53
bromobenzene...furan	−0.55	−2.82	−1.34	0.02	0.03	−0.05	−0.28	−0.86	−1.57
bromobenzene...pyridine	−1.37	−4.29	−2.67	0.04	0.10	−0.37	−9.46	−3.05	−35.11
bromobenzene...ammonia	−1.80	−3.13	−1.87	0.04	0.12	−0.55	−11.04	−3.70	−36.01
bromomethane...formaldehyde	0.01	−1.20	−0.10	—	—	—	—	—	—
2-bromopyrimidine...formaldehyde	−0.41	−1.68	−2.49	−0.06	0.12	−0.23	−1.00	−2.41	−7.74
5-bromo-pyrimidine...formaldehyde	−1.26	−2.72	−2.13	−0.28	0.00	−0.45	−1.25	−2.62	−2.62
1-bromo-1H-pyrrole...formaldehyde	−2.65	−4.40	−3.57	−0.78	−0.20	−1.18	−2.42	−3.33	−3.64
1-bromo-1H-imidazole...formaldehyde	−3.12	−4.91	−4.56	−1.03	−0.37	−1.44	−2.74	−3.85	−18.46
rms for bromo complexes relative to DFT ^f			3.36	3.85	4.68	2.93	12.30	3.87	51.02
rms for bromo complexes relative to MP2 ^f			2.89	8.76	9.50	7.88	10.43	2.92	47.47
iodobenzene...formaldehyde	−0.99	−2.56	−2.10	0.09	0.15	0.00	0.56	2.36	−18.44
iodobenzene...furan	−0.98	−3.73	−1.61	0.04	0.02	−0.03	1.47	4.80	−13.87
iodobenzene...pyridine	−2.85	−6.48	−3.40	0.09	0.12	−0.12	−1.31	3.03	−26.10
iodobenzene...ammonia	−3.29	−4.70	−2.45	0.08	0.11	−0.06	−3.29	1.67	−24.92
iodomethane...formaldehyde	−0.06	−2.08	−5.58	—	—	—	—	—	—
2-iodopyrimidine...formaldehyde	−1.00	−2.50	−2.91	0.03	0.20	−0.16	−0.53	1.64	−25.92
5-iodopyrimidine...formaldehyde	−1.95	−3.66	−3.07	−0.13	−0.04	−0.35	−0.51	1.32	−22.55
1-iodo-1H-pyrrole...formaldehyde	−3.97	−5.69	−4.76	−0.59	−0.38	−0.87	−1.84	1.01	−31.54
1-iodo-1H-imidazole...formaldehyde	−4.43	−6.23	−5.63	−0.80	0.73	−1.10	−2.27	0.51	−32.90
rms for iodo complexes relative to DFT ^f			3.10	7.15	8.20	6.62	4.72	13.07	63.99
rms for iodo complexes relative to MP2 ^f			4.58	12.71	13.60	12.18	10.48	18.98	58.59
total rms relative to DFT ^f			4.65	8.68	10.08	7.45	15.16	13.93	81.88
total rms relative to MP2 ^f			5.83	16.31	17.54	15.06	16.27	19.88	75.45

^a Binding energy E_{binding} is given by the expression: $E_{\text{binding}} = E_{\text{complex}} - E_{\text{halo molecule}} - E_{\text{Lewis base}}$. ^b Taken from our previous study.¹⁸ ^c Binding energies were calculated at the DFT/6-311+G**//DFT/6-311+G** level of theory using the aug-cc-pVDZ-PP basis set for the iodine and bromine atoms.

^d Binding energies were calculated at the MP2/6-311+G**//DFT/6-311+G** level of theory using the aug-cc-pVDZ-PP basis set for the iodine and bromine atoms. ^e No halogen bond formed. ^f Halomethane complex was not included in the rms estimation.

For the bromo complexes, the RM1 bond lengths agree well with the corresponding DFT data, except for the complexes of bromobenzene with pyridine and ammonia, for which they are short. For the iodo complexes, the RM1 halogen bond lengths are closer to the corresponding DFT data than the AM1 bond lengths, with rms errors of 1.42 and 3.05 Å, respectively. For the chloro and bromo complexes, the RM1 binding energies are farther from the corresponding DFT data than the AM1 binding energies. The rms errors in RM1 binding energies are 7.50, 12.30, and 4.72 kcal/mol for the chloro, bromo, and iodo complexes, respectively, relative to the corresponding DFT data.

The PM3 method is the best among the studied semiempirical methods for the chloro complexes, with rms error of just 0.39 Å relative to the corresponding DFT data. However, for bromo and

iodo complexes, the method does not differentiate between halogen bonds between the halogen atom and the different Lewis bases. For example, the average PM3 halogen bond lengths for the bromo and iodo complexes are 2.70 and 2.91 Å, respectively. Interestingly, for all the studied iodo complexes, the PM3 halogen bond lengths are short relative to the corresponding DFT data, but the PM3 binding energies are positive. Also, the PM3 binding energies are positive for all of the studied chlorobenzene and 2-chloropyrimidine complexes.

The PM6 method gives halogen bond lengths that are short for the chloro complexes and very short for the bromo and iodo complexes relative to the corresponding DFT data. A short bond length is associated with a higher binding energy; for the iodo complexes, binding energies exceed −13 kcal/mol. The overestimation in the

Table 4. Calculated Solvation Free Energies for Halobenzene Molecules Relative to Benzene

method	relative solvation free energy $\Delta\Delta G_{\text{solv}}$ (kcal/mol) ^a					
	Cl		Br		I	
	explicit solvent	implicit solvent	explicit solvent	implicit solvent	explicit solvent	implicit solvent
MM	0.30 (0.13)	−0.59 (0.08)	0.51 (0.16)	0.44 (0.08)	0.92 (0.19)	0.79 (0.24)
MNDO	0.97 (0.14)	1.13 (0.05)	1.38 (0.18)	0.57 (0.09)	1.63 (0.13)	2.15 (0.12)
AM1	0.82 (0.11)	−0.28 (0.04)	1.61 (0.16)	0.97 (0.09)	1.71 (0.26)	2.96 (0.10)
RM1	4.23 (0.18)	0.99 (0.06)	8.89 (0.23)	−2.20 (0.10)	−1.87 (0.31)	—
PM3	−8.30 (0.12)	—	0.60 (0.13)	0.89 (0.09)	−1.46 (0.29)	—
expt ^b	0.26		0.59		1.23 ^c	

^a Statistical uncertainties are given in parentheses. For statistical uncertainties and individual free energies, see the Supporting Information.

^b Experimental values are taken from ref 82. ^c The solvation energy of iodobenzene relative to benzene was calculated at the B3LYP/6-311+G**//B3LYP/6-311+G** level of theory; iodine atom was described using the aug-cc-pVDZ-PP basis set.

halogen bond binding energy is attributed to underestimated repulsion in the PM6 method.⁷⁹

A comparison between the performance of the semiempirical methods with MM data reveals that MM gives better halogen bond properties in terms of bond length and binding energy than do the studied semiempirical methods. Significantly, all the studied semiempirical methods show no halogen bond formation between halomethane with formaldehyde molecule, which is not the case for the MM level.

In conclusion, the AM1 method can be considered reliable for describing halogen bonding in chloro and bromo complexes, while the RM1 method is more reliable for doing so in iodo complexes. The other studied methods give inconsistent halogen bond lengths and/or bond energies relative to the corresponding DFT data.

Relative Solvation Free Energies. The long-range Coulomb potential and electrostatic element of solvation energy are affected by the charge description of the molecular system, and hence, the charge description needs to be as accurate as possible.^{80,81} The performance of the semiempirical methods in terms of charge-description accuracy for halogenated molecules, in particular halogen atoms, was investigated in the current study by calculating the solvation free energy of chloro-, bromo-, and iodobenzene molecules relative to benzene using the TI approach. Halobenzene and benzene molecules were treated with different methods, MM, MNDO, AM1, RM1, and PM3, with calculations performed in explicit and implicit GB water solvent. Table 4 lists the calculated relative solvation free energies. For comparison, experimental and pure MM data are also included. Energy derivatives and the statistical errors of the TI calculations are provided in the Supporting Information.

In explicit water solvent, the MNDO and AM1 solvation free energies of halobenzene molecules are positive in the order iodobenzene > bromobenzene > chlorobenzene, relative to benzene, and are higher than the corresponding experimental data, indicating that the MNDO and AM1 methods describe the atomic charges of the studied halogenated molecules correctly, but not accurately relative to experimental data.

In contrast, the RM1 and PM3 solvation free energies relative to benzene are negative for iodobenzene and chloro- and iodobenzene molecules, respectively, indicating that the RM1 and PM3 methods do not evaluate the correct charge description for the studied halobenzene molecules.

In implicit GB solvent, all the studied semiempirical methods give results that are inconsistent with the experimental data. The RM1 and PM3 methods do not retain the planarity of the iodobenzene and chloro- and iodobenzene molecules during molecular minimization, respectively, perhaps because the GB model is not well-parametrized for semiempirical method treatment of this molecular species.

Overall, for all the studied semiempirical methods, the calculated solvation free energies of halobenzene molecules relative to benzene are poor compared with the experimental data. Interestingly, the pure MM data are better than the results of the studied semiempirical methods, as found also for the geometrical optimizations and bond energy calculations of halogen-containing complexes.

GBSA Binding Energies. In evaluation of the appropriateness of the semiempirical treatment of the halogen bond in the hybrid QM/MM scheme, the molecular inhibition of CK2 protein with eight halobenzimidazole and -benzotriazole inhibitors was studied by performing pure MM-MD and hybrid QM/MM-MD simulations (length of 2 ns) advanced by a heating and equilibration phase (length of 550 ps). For the MM-MD simulations, an extra point of positive charge was placed on each inhibitor's halogen atom to represent the atom's positive cap. For the QM/MM-MD simulations, the most promising of the studied semiempirical methods, AM1, was used to describe the inhibitor.

To compare the relative performances of the MM-MD and QM/MM-MD simulations, a snapshot of the active site of CK2 protein complexed with 4,5,6,7-tetrahalo-1*H*-benzimidazole was taken after 1 ns of simulation. The results, given in Figure 4, indicate that the inhibitors are accommodated in the active site by the formation of a halogen bond with hinge-region Glu114 and Val116 residues.

Analysis of the MD trajectories provided perspective on the stability and properties of the halogen bond during the MD simulations. The halogen bond lengths of and the angle between the inhibitors' halogen atom and the Val116 residue's carboxyl oxygen atom measured over the MD trajectories are given in Table 5.

The average halogen bond length and angle measured over the QM/MM-MD trajectories are consistent with those measured over the MM-MD trajectories, with an overall bond length increase of 0.33 Å and average bond angle decrease of 8°. Significantly, relative to the MM-MD simulations, the QM/MM-MD simulations using the AM1 method for the QM region give a slightly long halogen

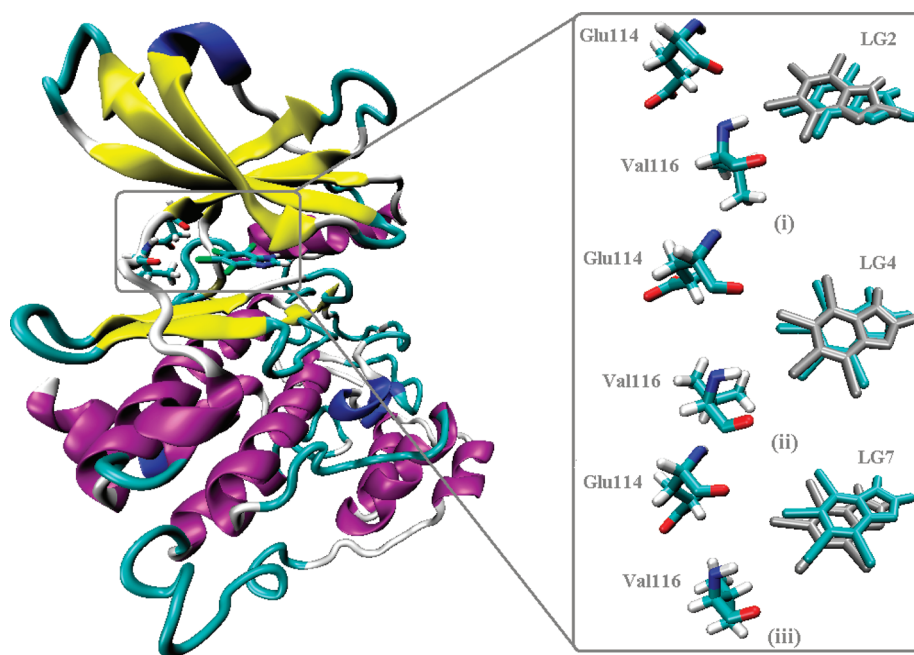


Figure 4. Snapshot taken at 1 ns during pure MM-MD (gray) and hybrid QM(AM1)/MM-MD (cyan) simulation of 4,5,6,7-tetra- (i) chloro-, (ii) bromo-, and (iii) iodo-1*H*-benzimidazole complexed to CK2 protein.

Table 5. Calculated Average Bond Length of and Bond Angle between Inhibitor's Halogen Atom and Val116 Residue's Carbonyl Oxygen

inhibitor	inhibitor's R ₂ /R ₃ ...Val116 residue's carbonyl oxygen ^a			
	average bond length (Å)		average bond angle (deg)	
	MM-MD	QM/MM-MD	MM-MD	QM/MM-MD
LG1	3.34	3.31	164.66	162.14
LG2	3.51	3.73	163.17	158.91
LG3	3.28	3.76	172.03	158.32
LG4	3.40	3.51	169.20	164.28
LG5	3.34	3.63	170.25	160.54
LG6	3.32	3.49	169.13	162.37
LG7	3.25	3.70	173.27	164.33
LG8	3.24	4.16	174.22	156.81

^a For definitions of R₂ and R₃, see Figure 2.

bond length for the chloro and bromo inhibitors and a long bond length for the iodo inhibitors. The latter result is consistent with our previous results for the geometrical optimization of iodine-containing complexes for which AM1 method gave long iodine...Lewis base contact relative to the corresponding DFT data (see Figure 3).

The MM-GBSA and QM/MM-GBSA binding energies were calculated using snapshots generated from the MM-MD and QM/MM-MD trajectories, respectively. The results are given in Table 6 and plotted in Figure 5. The energy components of the MM-GBSA and QM/MM-GBSA binding energies are provided in the Supporting Information.

The binding energies calculated using the pure MM-GBSA approach are in good agreement with the comparable experimental data, with a correlation coefficient R^2 of 0.90. Although,

Table 6. MM-GBSA and QM/MM-GBSA Binding Energies for the Studied Inhibitors with CK2 Protein

inhibitor	binding energy (kcal/mol)			
	MM-GBSA	QM/MM-GBSA	K_i (μ M)	ΔG_{expt}
LG1	−23.15	−25.61	6.00 ⁴⁹	−7.12
LG2	−22.78	−22.23	21.00 ⁸³	−6.37
LG3	−27.49	−20.27	0.40 ⁴⁶	−8.72
LG4	−27.23	−16.13	0.30 ⁴⁵	−8.89
LG5	−31.66	−19.60	0.23 ⁴⁵	−9.05
LG6	−32.56	−20.79	0.04 ⁴⁵	−10.08
LG7	−32.30	10.74	0.023 ⁴⁷	−10.41
LG8	−33.67	8.39	0.024 ⁴⁷	−10.38
R^2	0.90	−0.41		

the hybrid QM/MM-GBSA approach is considered to be more accurate than the classical MM force field approach, the hybrid QM/MM approach could not reproduce the experimental binding energies for the studied inhibitors and gave a correlation coefficient of −0.41. Similar poor performance of the hybrid QM/MM approach has been observed previously in studies on the binding energies of halogenated molecules.⁸⁴

To better understand the poor performance of the hybrid QM/MM approach, a further calculation was carried out in which the binding energies of the studied inhibitors were calculated using the MM-GBSA approach based on trajectories generated from the QM/MM-MD simulations. Figure 6i shows a plot of the results. The MM-GBSA//QM/MM-MD binding energies are closer to the corresponding experimental data than the QM/MM-GBSA//QM/MM-MD binding energies, with correlation factors improving from −0.41 for the QM/MM-GBSA approach to 0.81 for the MM-GBSA approach.

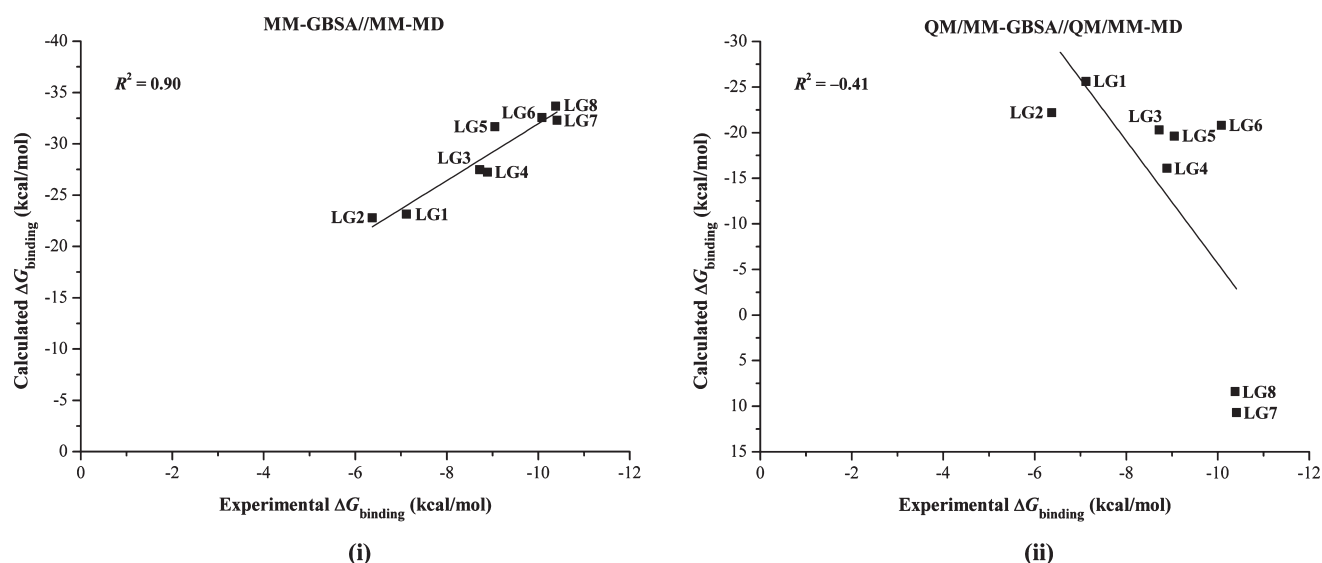


Figure 5. Calculated MM-GBSA and QM/MM-GBSA binding energies for the studied inhibitors with CK2 protein relative to the comparable experimental data.

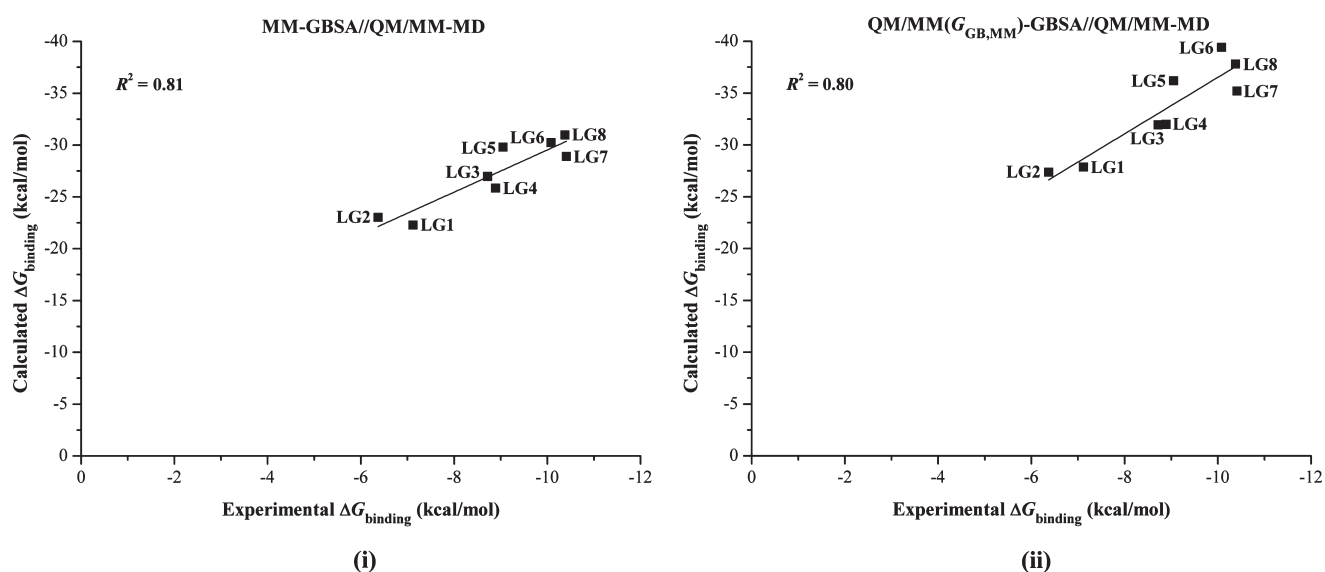


Figure 6. Binding energies of the studied inhibitors with CK2 protein relative to the experimental data calculated by two approaches based on the QM/MM-MD trajectories: (i) the MM-GBSA approach and (ii) the QM/MM-GBSA approach, with the $G_{\text{GB,QM/MM}}$ solvation energy term replaced with the corresponding the $G_{\text{GB,MM}}$ term.

The poor binding energy results given by the QM/MM-GBSA approach for the studied inhibitors can be attributed to the poor GB solvation energy of the QM region, as observed previously in the solvation free energy calculations of the halobenzene molecules relative to benzene in implicit GB solvent. Therefore, the G_{GB} solvation energy term in the QM/MM-GBSA binding energy calculations was replaced with the corresponding G_{GB} solvation energy term in the MM-GBSA calculations, thereby improving the calculated binding energy and giving a correlation coefficient of 0.80 (Figure 6ii). The success of this replacement shows that the semiempirical methods are reliable for treating QM/MM interactions electrostatically. At the same time, reparameterization of the GB model for the semiempirical methods is mandatory to ensure

the accuracy of the solvation energy term in implicit solvent at a semiempirical level.

Comparison of the calculated MM-GBSA//MM-MD and QM($G_{\text{GB,MM}}$)/MM-GBSA//QM/MM-MD binding energies indicates that the pure MM approach, with the σ -hole on the halogen atom represented by a positively charged extra point in the classical MM force field, performs better than the hybrid QM/MM approach.

Finally, it should be mentioned that the better performance of semiempirical methods in describing CK2 protein kinase inhibitors involving halogen bonds was achieved by using an advanced semiempirical quantum mechanical method, such as PM6-DH2X, combined with accurate quantum solvation model.⁸⁵

CONCLUSION

The current study was carried out to assess the performance of several semiempirical methods in handling halogen bonding.

In geometrical optimizations and binding energy calculations of 27 halogen-containing molecules complexed with various Lewis bases, the following was observed. For chloro and bromo complexes, the AM1 method gives results that are in good agreement with the corresponding DFT data. For iodo complexes, the RM1 method gives better results than the AM1 method, whose halogen bond lengths are long. For all of the complexes, the MNDO and MNDO-*d* methods erroneously show no halogen bond between the halogen atom and the Lewis base, and the PM3 and PM6 methods give halogen bond lengths that are short relative to the corresponding DFT data.

In calculations of the solvation free energies of halobenzene molecules relative to benzene in explicit water solvent, the MNDO and AM1 methods give results in closer agreement with the experimental data than the other studied methods.

In evaluations of the appropriateness of the AM1 semiempirical method toward halogen bonding using a QM/MM approach, results were improved by replacing the $G_{\text{GB,QM/MM}}$ solvation energy term with the corresponding $G_{\text{GB,MM}}$ term. However, overall, a pure MM approach with inclusion of an extra point of positive charge on the halogen atom gives better results than the QM/MM approach.

ASSOCIATED CONTENT

S Supporting Information. Information concerning the energy derivative of the relative solvation free energies and the energy component of the GBSA binding energies. This material is available free of charge via the Internet at <http://pubs.acs.org>

AUTHOR INFORMATION

Corresponding Author

*E-mail: m.ibrahim@compchem.net

ACKNOWLEDGMENT

The author thanks the use of the UK NGS in carrying out this work, and in particular the STFC eScience Centre (RAL) for providing computational support for Gaussian and AMBER packages.

REFERENCES

- (1) Brammer, L. *Hydrogen Bonds in Inorganic Chemistry: Application to Crystal Design*; John Wiley & Sons: New York, 2003.
- (2) Lu, Y.; Wang, Y.; Zhu, W. Nonbonding interactions of organic halogens in biological systems: Implications for drug discovery and biomolecular design. *Phys. Chem. Chem. Phys.* **2010**, *12*, 4543–4551.
- (3) Lu, Y.; Shi, T.; Wang, Y.; Yang, H.; Yan, X.; Luo, X.; Jiang, H.; Zhu, W. Halogen bonding—A novel interaction for rational drug design?. *J. Med. Chem.* **2009**, *52*, 2854–2862.
- (4) Matta, C. F.; Hernández-Trujillo, J.; Tang, T.-H.; Bader, R. F. W. Hydrogen—hydrogen bonding: A stabilizing interaction in molecules and crystals. *Chem.—Eur. J.* **2003**, *9*, 1940–1951.
- (5) Desiraju, G. R. Hydrogen bridges in crystal engineering: Interactions without borders. *Acc. Chem. Res.* **2002**, *35*, 565–573.
- (6) Lee, S.; Mallik, A. B.; Fredrickson, D. C. Dipolar—dipolar interactions and the crystal packing of nitriles, ketones, aldehydes, and $\text{C}(\text{sp}^2)$ —F groups. *Cryst. Growth Des.* **2003**, *4*, 279–290.

- (7) Clark, T.; Hennemann, M.; Murray, J.; Politzer, P. Halogen bonding: The σ -hole. *J. Mol. Model.* **2007**, *13*, 291–296.
- (8) Fourmigué, M. Halogen bonding: Recent advances. *Curr. Opin. Solid State Mater. Sci.* **2009**, *13*, 36–45.
- (9) Politzer, P.; Lane, P.; Concha, M.; Ma, Y.; Murray, J. An overview of halogen bonding. *J. Mol. Model.* **2007**, *13*, 305–311.
- (10) Auffinger, P.; Hays, F. A.; Westhof, E.; Ho, P. S. Halogen bonds in biological molecules. *Proc. Natl. Acad. Sci. U. S. A.* **2004**, *101*, 16789–16794.
- (11) Politzer, P.; Murray, J. S.; Clark, T. Halogen bonding: An electrostatically-driven highly directional noncovalent interaction. *Phys. Chem. Chem. Phys.* **2010**, *12*, 7748–7757.
- (12) Gavezzotti, A. Non-conventional bonding between organic molecules. The ‘halogen bond’ in crystalline systems. *Mol. Phys.* **2008**, *106*, 1473–1485.
- (13) Zhou, P.; Lv, J.; Zou, J.; Tian, F.; Shang, Z. Halogen—water—hydrogen bridges in biomolecules. *J. Struct. Biol.* **2010**, *169*, 172–182.
- (14) Amezcua, N. J. M.; Pamies, S. C.; Peruchena, N. I. M.; Sosa, G. L. Halogen bonding: A study based on the electronic charge density. *J. Phys. Chem. A* **2009**, *114*, 552–562.
- (15) Palusiak, M. On the nature of halogen bond—The Kohn—Sham molecular orbital approach. *J. Mol. Struct. THEOCHEM* **2010**, *945*, 89–92.
- (16) Bui, T. T. T.; Dahanoui, S.; Lecomte, C.; Desiraju, G. R.; Espinosa, E. The nature of halogen...Halogen interactions: A model derived from experimental charge-density analysis. *Angew. Chem., Int. Ed.* **2009**, *48*, 3838–3841.
- (17) Metrangola, P.; Neukirch, H.; Pilati, T.; Resnati, G. Halogen bonding based recognition processes: A world parallel to hydrogen bonding. *Acc. Chem. Res.* **2005**, *38*, 386–395.
- (18) Ibrahim, M. A. A. Molecular mechanical study of halogen bonding in drug discovery. *J. Comput. Chem.* **2011**, *32*, 2564–2574.
- (19) Field, M. J.; Bash, P. A.; Karplus, M. A combined quantum mechanical and molecular mechanical potential for molecular dynamics simulations. *J. Comput. Chem.* **1990**, *11*, 700–733.
- (20) Walker, R. C.; Crowley, M. F.; Case, D. A. The implementation of a fast and accurate QM/MM potential method in amber. *J. Comput. Chem.* **2008**, *29*, 1019–1031.
- (21) Burk, P.; Herodes, K.; Koppel, I.; Koppel, I. Critical test of PM3-calculated proton affinities. *Int. J. Quantum Chem.* **1993**, *48*, 633–641.
- (22) Zerner, M. C. Semiempirical molecular orbital methods. In *Reviews in Computational Chemistry*; Lipkowitz, K. B., Boyd, D. B., Eds.; John Wiley & Sons, Inc.: Hoboken, NJ, 2007; Vol. 2, pp 313–365.
- (23) Stewart, J. Application of the PM6 method to modeling proteins. *J. Mol. Model.* **2009**, *15*, 765–805.
- (24) Stewart, J. Application of the PM6 method to modeling the solid state. *J. Mol. Model.* **2008**, *14*, 499–535.
- (25) Yatsenko, A. V.; Paseshnichenko, K. A. A semi-empirical electrostatic potential in the studies of molecular crystals. *Chem. Phys.* **2000**, *262*, 293–301.
- (26) Repasky, M. P.; Chandrasekhar, J.; Jorgensen, W. L. Improved semiempirical heats of formation through the use of bond and group equivalents. *J. Comput. Chem.* **2002**, *23*, 498–510.
- (27) Stewart, J. J. P. Optimization of parameters for semiempirical methods II. Applications. *J. Comput. Chem.* **1989**, *10*, 221–264.
- (28) Dewar, M. J. S.; Dieter, K. M. Evaluation of AM1 calculated proton affinities and deprotonation enthalpies. *J. Am. Chem. Soc.* **1986**, *108*, 8075–8086.
- (29) Cui, Q.; Elstner, M.; Karplus, M. A theoretical analysis of the proton and hydride transfer in liver alcohol dehydrogenase (LADH). *J. Phys. Chem. B* **2002**, *106*, 2721–2740.
- (30) Truhlar, D. G.; Gao, J.; Alhambra, C.; Garcia-Viloca, M.; Corchado, J.; Sánchez, M. L.; Villá, J. The incorporation of quantum effects in enzyme kinetics modeling. *Acc. Chem. Res.* **2002**, *35*, 341–349.
- (31) Hammes-Schiffer, S. Hydrogen tunneling and protein motion in enzyme reactions. *Acc. Chem. Res.* **2005**, *39*, 93–100.

- (32) Gao, J.; Truhlar, D. G. Quantum mechanical methods for enzyme kinetics. *Annu. Rev. Phys. Chem.* **2002**, *53*, 467–505.
- (33) Bonati, L.; Cosentino, U.; Fraschini, E.; Moro, G.; Pitea, D. Molecular electrostatic potential of substituted aromatic compounds: Factors affecting the differences between ab initio and semiempirical results. *J. Comput. Chem.* **1992**, *13*, 842–850.
- (34) Cummins, P. L.; Gready, J. E. The electrostatic potential in the semiempirical molecular orbital approximation. *Chem. Phys. Lett.* **1994**, *225*, 11–17.
- (35) Alkorta, I.; Villar, H. O.; Arteca, G. A. Comparative study between ab initio and semiempirical electrostatic potentials on molecular surfaces. *J. Comput. Chem.* **1993**, *14*, 530–540.
- (36) Besler, B. H.; Merz, K. M.; Kollman, P. A. Atomic charges derived from semiempirical methods. *J. Comput. Chem.* **1990**, *11*, 431–439.
- (37) Ferenczy, G. G.; Reynolds, C. A.; Richards, W. G. Semiempirical AM1 electrostatic potentials and AM1 electrostatic potential derived charges: A comparison with ab initio values. *J. Comput. Chem.* **1990**, *11*, 159–169.
- (38) Luque, F. J.; Illas, F.; Orozco, M. Comparative study of the molecular electrostatic potential obtained from different wavefunctions. Reliability of the semiempirical mndo wavefunction. *J. Comput. Chem.* **1990**, *11*, 416–430.
- (39) Rodríguez, J.; Manaut, F.; Sanz, F. Quantitative comparison of molecular electrostatic potential distributions from several semiempirical and ab initio wave functions. *J. Comput. Chem.* **1993**, *14*, 922–927.
- (40) Anisimov, V. M.; Anikin, N.; Bugaenko, V.; Bobrikov, V.; Andreyev, A. Accuracy assessment of semiempirical molecular electrostatic potential of proteins. *Theor. Chem. Acc. Theor. Comput. Model (Theor. Chim. Acta)* **2003**, *109*, 213–219.
- (41) Reynolds, C. A.; Ferenczy, G. G.; Richards, W. G. Methods for determining the reliability of semiempirical electrostatic potentials and potential derived charges. *J. Mol. Struct. THEOCHEM* **1992**, *256*, 249–269.
- (42) Bakowies, D.; Thiel, W. Semiempirical treatment of electrostatic potentials and partial charges in combined quantum mechanical and molecular mechanical approaches. *J. Comput. Chem.* **1996**, *17*, 87–108.
- (43) Bakowies, D.; Thiel, W. Hybrid models for combined quantum mechanical and molecular mechanical approaches. *J. Phys. Chem.* **1996**, *100*, 10580–10594.
- (44) Pinna, L. A. Protein kinase CK2: A challenge to canons. *J. Cell. Sci.* **2002**, *115*, 3873–3878.
- (45) Pagano, M. A.; Andrzejewska, M.; Ruzzene, M.; Sarno, S.; Cesaro, L.; Bain, J.; Elliott, M.; Meggio, F.; Kazimierczuk, Z.; Pinna, L. A. Optimization of protein kinase CK2 inhibitors derived from 4,5,6,7-tetrabromobenzimidazole. *J. Med. Chem.* **2004**, *47*, 6239–6247.
- (46) Battistutta, R.; Mazzorana, M.; Sarno, S.; Kazimierczuk, Z.; Zanotti, G.; Pinna, L. A. Inspecting the structure-activity relationship of protein kinase CK2 inhibitors derived from tetrabromo-benzimidazole. *Chem. Biol.* **2005**, *12*, 1211–1219.
- (47) Gianoncelli, A.; Cozza, G.; Orzeszko, A.; Meggio, F.; Kazimierczuk, Z.; Pinna, L. A. Tetraiodobenzimidazoles are potent inhibitors of protein kinase CK2. *Bioorg. Med. Chem.* **2009**, *17*, 7281–7289.
- (48) Zien, P.; Duncan, J. S.; Skierski, J.; Bretner, M.; Litchfield, D. W.; Shugar, D. Tetrabromobenzotriazole (TBBt) and tetrabromobenzimidazole (TBBz) as selective inhibitors of protein kinase CK2: Evaluation of their effects on cells and different molecular forms of human CK2. *BBA-Proteins Proteom.* **2005**, *1754*, 271–280.
- (49) Szyszka, R.; Grankowski, N.; Felczak, K.; Shugar, D. Halogenated benzimidazoles and benzotriazoles as selective inhibitors of protein kinases CK-I and CK-II from *Saccharomyces cerevisiae* and other sources. *Biochem. Biophys. Res. Commun.* **1995**, *208*, 418–424.
- (50) Dobrowolska, G.; Muszynska, G.; Shugar, D. Benzimidazole nucleoside analogues as inhibitors of plant (maize seedling) casein kinases. *BBA-Protein Struct. Mol. Enzymol.* **1991**, *1080*, 221–226.
- (51) Andrzejewska, M.; Pagano, M. A.; Meggio, F.; Brunati, A. M.; Kazimierczuk, Z. Polyhalogenobenzimidazoles: Synthesis and their inhibitory activity against casein kinases. *Bioorg. Med. Chem.* **2003**, *11*, 3997–4002.
- (52) Mazzorana, M.; Pinna, L.; Battistutta, R. A structural insight into CK2 inhibition. *Mol. Cell. Biochem.* **2008**, *316*, 57–62.
- (53) Dewar, M. J. S.; Thiel, W. Ground states of molecules. 39. MNDO results for molecules containing hydrogen, carbon, nitrogen, and oxygen. *J. Am. Chem. Soc.* **1977**, *99*, 4907–4917.
- (54) Dewar, M. J. S.; Thiel, W. Ground states of molecules. 38. The MNDO method. Approximations and parameters. *J. Am. Chem. Soc.* **1977**, *99*, 4899–4907.
- (55) Thiel, W.; Voityuk, A. A. Extension of MNDO to d orbitals: Parameters and results for the second-row elements and for the zinc group. *J. Phys. Chem.* **1996**, *100*, 616–626.
- (56) Thiel, W.; Voityuk, A. A. Extension of the MNDO formalism to d orbitals: Integral approximations and preliminary numerical results. *Theor. Chem. Accounts Theor. Comput. Model (Theor. Chim. Acta)* **1992**, *81*, 391–404.
- (57) Dewar, M. J. S.; Zoebisch, E. G. Extension of AM1 to the halogens. *J. Mol. Struct. THEOCHEM* **1988**, *180*, 1–21.
- (58) Dewar, M. J. S.; Zoebisch, E. G.; Healy, E. F.; Stewart, J. J. P. AM1: A new general purpose quantum mechanical molecular model. *J. Am. Chem. Soc.* **1985**, *107*, 3902–3909.
- (59) Rocha, G. B.; Freire, R. O.; Simas, A. M.; Stewart, J. J. P. RM1: A reparameterization of AM1 for H, C, N, O, P, S, F, Cl, Br, and I. *J. Comput. Chem.* **2006**, *27*, 1101–1111.
- (60) Stewart, J. J. P. Optimization of parameters for semiempirical methods I. Method. *J. Comput. Chem.* **1989**, *10*, 209–220.
- (61) Stewart, J. Optimization of parameters for semiempirical methods V: Modification of NDDO approximations and application to 70 elements. *J. Mol. Model.* **2007**, *13*, 1173–1213.
- (62) Stewart, J. J. P. MOPAC2009; Stewart Computational Chemistry: Colorado Springs, CO, 2008.
- (63) Becke, A. D. Density-functional exchange-energy approximation with correct asymptotic behavior. *Phys. Rev. A* **1988**, *38*, 3098–3100.
- (64) Lee, C.; Yang, W.; Parr, R. G. Development of the Colle–Salvetti correlation-energy formula into a functional of the electron density. *Phys. Rev. B* **1988**, *37*, 785–789.
- (65) Adamo, C.; Barone, V. Exchange functionals with improved long-range behavior and adiabatic connection methods without adjustable parameters: The mPW and mPW1PW models. *J. Chem. Phys.* **1998**, *108*, 664–675.
- (66) Yun-Xiang, L.; Jian-Wei, Z.; Ji-Cai, F.; Wen-Na, Z.; Yong-Jun, J.; Qing-Sen, Y. Ab initio calculations on halogen-bonded complexes and comparison with density functional methods. *J. Comput. Chem.* **2009**, *30*, 725–732.
- (67) Dunning, J. T. H. Gaussian basis sets for use in correlated molecular calculations. I. The atoms boron through neon and hydrogen. *J. Chem. Phys.* **1989**, *90*, 1007–1023.
- (68) Woon, D. E.; Dunning, J. T. H. Gaussian basis sets for use in correlated molecular calculations. III. The atoms aluminum through argon. *J. Chem. Phys.* **1993**, *98*, 1358–1371.
- (69) Krishnan, R.; Binkley, J. S.; Seeger, R.; Pople, J. A. Self-consistent molecular orbital methods. XX. A basis set for correlated wave functions. *J. Chem. Phys.* **1980**, *72*, 650–654.
- (70) Bayly, C. I.; Cieplak, P.; Cornell, W.; Kollman, P. A. A well-behaved electrostatic potential based method using charge restraints for deriving atomic charges: The RESP model. *J. Phys. Chem.* **1993**, *97*, 10269–10280.
- (71) Frisch, M. J.; Trucks, G. W.; Schlegel, H. B.; Scuseria, G. E.; Robb, M. A.; Cheeseman, J. R.; Montgomery, J. A., Jr., T., V.; Kudin, K. N.; Burant, J. C.; Millam, J. M.; Iyengar, S. S.; Tomasi, J.; Barone, V.; Mennucci, B.; Cossi, M.; Scalmani, G.; Rega, N.; Petersson, G. A.; Nakatsuji, H.; Hada, M.; Ehara, M.; Toyota, K.; Fukuda, R.; Hasegawa, J.; Ishida, M.; Nakajima, T.; Honda, Y.; Kitao, O.; Nakai, H.; Klene, M.; Li, X.; Knox, J. E.; Hratchian, H. P.; Cross, J. B.; Bakken, V.; Adamo, C.; Jaramillo, J.; Gomperts, R.; Stratmann, R. E.; Yazyev, O.; Austin, A. J.; Cammi, R.; Pomelli, C.; Ochterski, J. W.; Ayala, P. Y.; Morokuma, K.; Voth, G. A.; Salvador, P.; Dannenberg, J. J.; Zakrzewski, V. G.; Dapprich,

S.; Daniels, A. D.; Strain, M. C.; Farkas, O.; Malick, D. K.; Rabuck, A. D.; Raghavachari, K.; Foresman, J. B.; Ortiz, J. V.; Cui, Q.; Baboul, A. G.; Clifford, S.; Cioslowski, J.; Stefanov, B. B.; Liu, G.; Liashenko, A.; Piskorz, P.; Komaromi, I.; Martin, R. L.; Fox, D. J.; Keith, T.; Al-Laham, M. A.; Peng, C. Y.; Nanayakkara, A.; Challacombe, M.; Gill, P. M. W.; Johnson, B.; Chen, W.; Wong, M. W.; Gonzalez, C.; Pople, J. A. *Gaussian 03*; Gaussian, Inc.: Wallingford, CT, 2004.

(72) Kollman, P. Free energy calculations: Applications to chemical and biochemical phenomena. *Chem. Rev.* **1993**, 93, 2395–2417.

(73) Straatsma, T. P.; McCammon, J. A. Multiconfiguration thermodynamic integration. *J. Chem. Phys.* **1991**, 95, 1175–1188.

(74) Case, D. A.; Darden, T. A.; T., E. Cheatham, I.; Simmerling, C. L.; Wang, J.; Duke, R. E.; Luo, R.; Crowley, M.; Walker, R. C.; Zhang, W.; Merz, K. M.; Wang, B.; Hayik, S.; Roitberg, A.; Seabra, G.; Kolosváry, I.; Wong, K. F.; Paesani, F.; Vanicek, J.; Wu, X.; Brozell, S. R.; Steinbrecher, T.; Gohlke, H.; Yang, L.; Tan, C.; Mongan, J.; Hornak, V.; Cui, G.; Mathews, D. H.; Seetin, M. G.; Sagui, C.; Babin, V.; Kollman, P. A. *AMBER 10*; University of California: San Francisco, CA, 2008.

(75) Jorgensen, W. L.; Chandrasekhar, J.; Madura, J. D.; Impey, R. W.; Klein, M. L. Comparison of simple potential functions for simulating liquid water. *J. Chem. Phys.* **1983**, 79, 926–935.

(76) Wang, J.; Wolf, R. M.; Caldwell, J. W.; Kollman, P. A.; Case, D. A. Development and testing of a general amber force field. *J. Comput. Chem.* **2004**, 25, 1157–1174.

(77) Hornak, V.; Abel, R.; Okur, A.; Strockbine, B.; Roitberg, A.; Simmerling, C. Comparison of multiple amber force fields and development of improved protein backbone parameters. *Proteins: Struct. Funct. Bioinf.* **2006**, 65, 712–725.

(78) Sitkoff, D.; Sharp, K. A.; Honig, B. Accurate calculation of hydration free energies using macroscopic solvent models. *J. Phys. Chem.* **1994**, 98, 1978–1988.

(79) Rezáč, J.; Hobza, P. A halogen-bonding correction for the semiempirical PM6 method. *Chem. Phys. Lett.* **2011**, 506, 286–289.

(80) Pascual-Ahuir, J. L.; Silla, E.; Tomasi, J.; Bonaccorsi, R. Electrostatic interaction of a solute with a continuum. Improved description of the cavity and of the surface cavity bound charge distribution. *J. Comput. Chem.* **1987**, 8, 778–787.

(81) Tannor, D. J.; Marten, B.; Murphy, R.; Friesner, R. A.; Sitkoff, D.; Nicholls, A.; Honig, B.; Ringnalda, M.; Goddard, W. A. Accurate first principles calculation of molecular charge distributions and solvation energies from *ab initio* quantum mechanics and continuum dielectric theory. *J. Am. Chem. Soc.* **1994**, 116, 11875–11882.

(82) Cabani, S.; Gianni, P.; Mollica, V.; Lepori, L. Group contributions to the thermodynamic properties of non-ionic organic solutes in dilute aqueous solution. *J. Solution Chem.* **1981**, 10, 563–595.

(83) Zien, P.; Bretner, M.; Zastapilo, K.; Szyzka, R.; Shugar, D. Selectivity of 4,5,6,7-tetrabromobenzimidazole as an ATP-competitive potent inhibitor of protein kinase CK2 from various sources. *Biochem. Biophys. Res. Commun.* **2003**, 306, 129–133.

(84) Retegan, M.; Milet, A.; Jamet, H. Exploring the binding of inhibitors derived from tetrabromobenzimidazole to the CK2 protein using a QM/MM-PB/SA approach. *J. Chem. Inf. Model.* **2009**, 49, 963–971.

(85) Dobeš, P.; Rezáč, J.; Fanfrlík, J.; Otyepka, M.; Hobza, P. Semiempirical quantum mechanical method PM6-DH2X describes the geometry and energetics of CK2-inhibitor complexes involving halogen bonds well, while the empirical potential fails. *J. Phys. Chem. B* **2011**, 115, 8581–8589.